International Tables for Crystallography (2006). Vol. C, Section 2.2.2, pp. 29–30.

geometry is an efficient way of measuring a large number of relp's between $d^*_{\max}$ and $d^*_{\max}/2$ as single-wavelength spots.

The above is a brief description of the overall multiplicity distribution. For a given relp, even of simple *hkl* values, lying on a ray of several relp's (multiples of *hkl*), a suitable choice of crystal orientation can yield a single-wavelength spot. Consider, for example, a spot of multiplicity 5. The outermost relp can be recorded at long wavelength with the inner relp's on the ray excluded since they need λ's greater than $\lambda_{\max}$ (Fig. 2.2.1.3). Alternatively, by rotating the sample, the innermost relp can be measured uniquely at short wavelength with the outer relp's excluded (they require λ's shorter than $\lambda_{\min}$). Hence, in Laue geometry several orientations are needed to recover virtually all relp's as singles. The multiplicity distribution is shown in Fig. 2.2.1.4 as a function of $\lambda_{\max}/\lambda_{\min}$ (with the corresponding values of $\delta\lambda/\lambda_{\rm mean}$).

2.2.1.4. *Angular distribution of reflections in Laue diffraction*

There is an interesting variation in the angular separations of Laue reflections that shows up in the spatial distributions of spots on a detector plane (Cruickshank, Helliwell & Moffat, 1991). There are two main aspects to this distribution, which are general and local. The general aspects refer to the diffraction pattern as a whole and the local aspects to reflections in a particular zone of diffraction spots.

The general features include the following. The spatial density of spots is everywhere proportional to $1/D^2$, where D is the crystal-to-detector distance, and to $1/V^*$, where V^* is the reciprocal-cell volume. There is also though a substantial variation in spatial density with diffraction angle θ; a prominent maximum occurs at

$$\theta_c = \sin^{-1}(\lambda_{\min} d^*_{\max}/2). \qquad (2.2.1.9)$$

Local aspects of these patterns particularly include the prominent conics on which Laue reflections lie. That is, the local spatial distribution is inherently one-dimensional in character. Between multiple reflections (nodals), there is always at least one single and therefore nodals have a larger angular separation from their nearest neighbours. The blank area around a nodal in a Laue pattern (Fig. 2.2.1.2) has been noted by Jeffery (1958). The smallest angular separations, and therefore spatially overlapped cases, are associated with single Laue reflections. Thus, the reflections involved in energy overlaps – the multiples – form a set largely distinct, except at short crystal-to-detector distances, from those involved in spatial overlaps, which are mostly singles (Helliwell, 1985).

From a knowledge of the form of the angular distribution, it is possible, *e.g.* from the gaps bordering conics, to estimate $d^*_{\max}$ and $\lambda_{\min}$. However, a development of this involving gnomonic projections can be even more effective (Cruickshank, Carr & Harding, 1992).

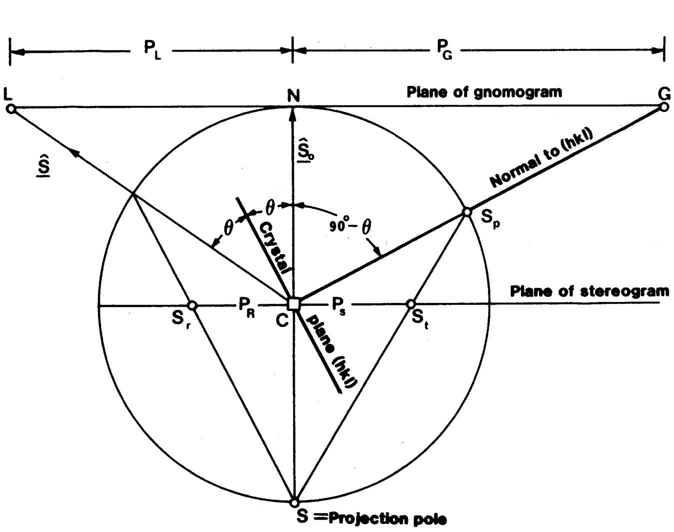

Fig. 2.2.1.5. Geometrical principles of the spherical, stereographic, gnomonic, and Laue projections. From Evans & Lonsdale (1959).

2.2.1.5. *Gnomonic and stereographic transformations*

A useful means of transformation of the flat-film Laue pattern is the gnomonic projection. This converts the pattern of spots lying on curved arcs to points lying on straight lines. The stereographic projection is also used. Fig. 2.2.1.5 shows the graphical relationships involved [taken from *International Tables*, Vol. II (Evans & Lonsdale, 1959)], for the case of a Laue pattern recorded on a plane film, between the incident-beam direction *SN*, which is perpendicular to a film plane and the Laue spot L and its spherical, stereographic, and gnomonic points S_p, S_t and G and the stereographic projection S_r of the reflected beams. If the radius of the sphere of projection is taken equal to D, the crystal-to-film distance, then the planes of the gnomonic projection and of the film coincide. The lines producing the various projection poles for any given crystal plane are coplanar with the incident and reflected beams. The transformation equations are

$$P_L = D\tan 2\theta \qquad (2.2.1.10)$$

$$P_G = D\cot\theta \qquad (2.2.1.11)$$

$$P_S = D\frac{\cos\theta}{(1+\sin\theta)} \qquad (2.2.1.12)$$

$$P_R = D\tan\theta. \qquad (2.2.1.13)$$

2.2.2. Monochromatic methods

In this section and those that follow, which deal with monochromatic methods, the convention is adopted that the Ewald sphere takes a radius of unity and the magnitude of the reciprocal-lattice vector is λ/d. This is not the convention used in the Laue section above.

Some historical remarks are useful first before progressing to discuss each monochromatic geometry in detail. The original rotation method (for example, see Bragg, 1949) involved a rotation of a perfectly aligned crystal of 360°. For reasons of relatively poor collimation of the X-ray beam, leading to spot-to-spot overlap, and background build-up, Bernal (1927) introduced the oscillation method whereby a repeated, limited, angular range was used to record one pattern and a whole series of contiguous ranges on different film exposures were collected to provide a large angular coverage overall. In a different solution to the same problem, Weissenberg (1924) utilized a layer-line screen to record only one layer line but allowed a full rotation of the crystal but now coupled to translation of the detector, thus avoiding spot-to-spot overlap. Again, several exposures were needed, involving one layer line collected on each exposure. The advent of synchrotron radiation with very high intensity allows small beam sizes at the sample to be practicable, thus simultaneously creating small diffraction spots and minimizing background scatter. The very fine collimation of the synchrotron beam keeps the diffraction-spot sizes small as they traverse their path to the detector plane.

The terminology used today for different methods is essentially the same as originally used except that the rotation method now tends to mean limited angular ranges (instead of 360°) per diffraction photograph/image. The Weissenberg method in its modern form now employed at a synchrotron is a screenless technique with limited angular range but still with detector translation coupled to crystal rotation.

2.2.2.1. *Monochromatic still exposure*

In a monochromatic still exposure, the crystal is held stationary and a near-zero wavelength-bandpass (*e.g.* $\delta\lambda/\lambda = 0.001$) beam impinges on it. For a small-molecule crystal, there are few diffraction spots. For a protein crystal, there are many (several hundred), because of the much denser reciprocal lattice. The actual number of stimulated relp's depends on the reciprocal-cell parameters, the size of the mosaic spread of the crystal, the angular beam divergence as well as the small, but finite, spectral spread, $\delta\lambda/\lambda$. Diffraction spots are only partially stimulated instead of fully integrated over wavelength, as in the Laue method, or over an angular rotation (the rocking width) in rotating-crystal monochromatic methods.

The diffraction spots lie on curved arcs where each curve corresponds to the intersection with a film of a cone. With a flat film the intersections are conic sections. The curved arcs are obviously recognizable for the protein crystal case where there are a large number of spots.

2.2.2.2. *Crystal setting*

Crystal setting follows the procedure given in Subsection 2.2.1.2 whereby angular mis-setting angles are given by equation (2.2.1.3). When viewed down a zone axis, the pattern on a flat film or electronic area detector has the appearance of a series of concentric circles. For example, with the beam parallel to $[00\bar{1}]$, the first circle corresponds to $l = 1$, the second to $l = 2$, *etc*. The radius of the first circle R is related to the interplanar spacing between the ($hk0$) and ($hk1$) planes, *i.e.* λ/c (in this example), through θ, by the formulae

$$\tan 2\theta = R/D; \quad \cos 2\theta = 1 - \lambda/c. \qquad (2.2.2.1)$$

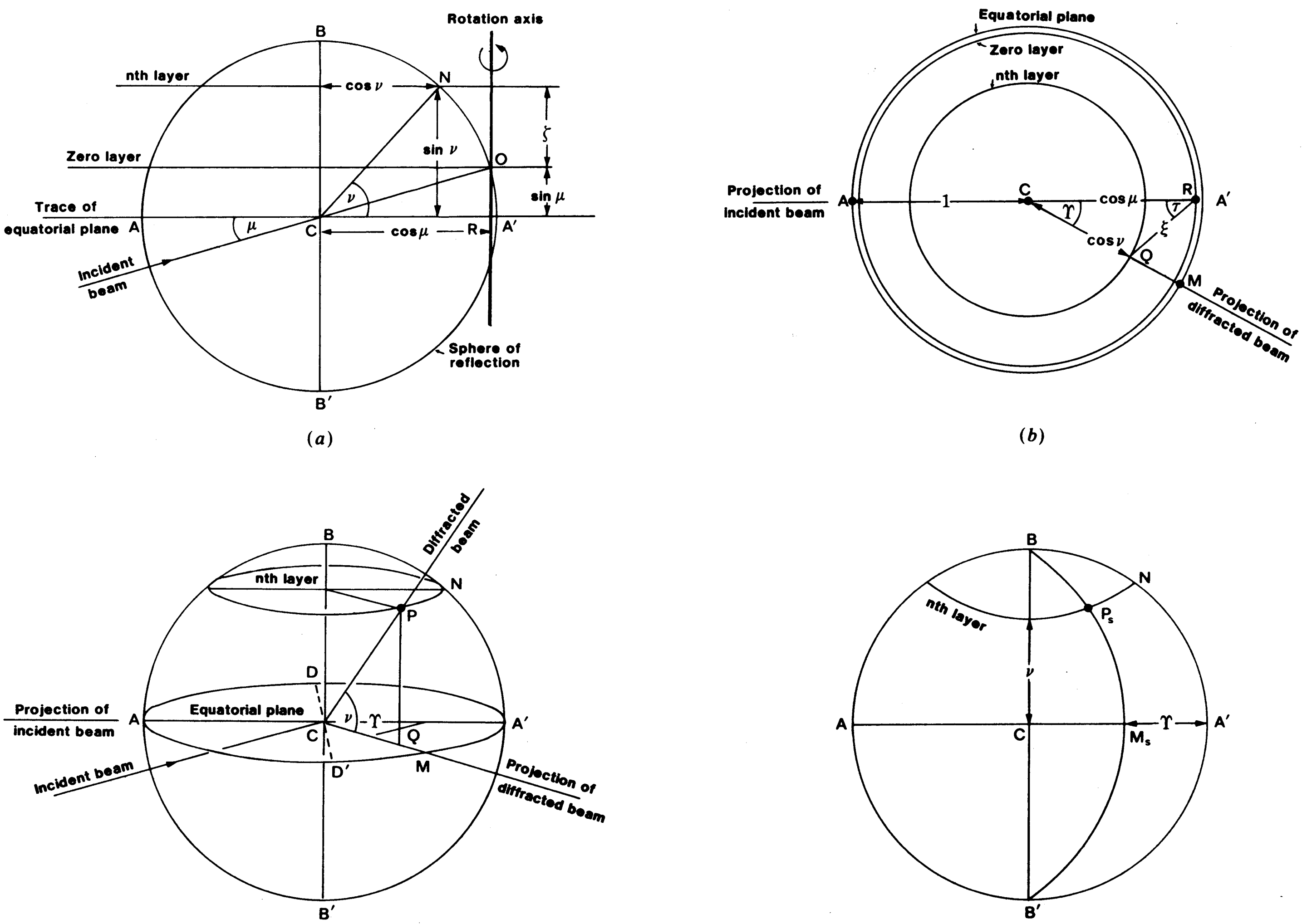

Fig. 2.2.3.1. (*a*) Elevation of the sphere of reflection. *O* is the origin of the reciprocal lattice. *C* is the centre of the Ewald sphere. The incident beam is shown in the plane. (*b*) Plan of the sphere of reflection. *R* is the projection of the rotation axis on the equatorial plane. (*c*) Perspective diagram. *P* is the relp in the reflection position with the cylindrical coordiantes ζ, ξ, φ. The angular coordinates of the diffracted beam are ν, Υ. (*d*) Stereogram to show the direction of the diffracted beam, ν, Υ, with DD', normal to the incident beam and in the equatorial plane, as the projection diameter. From Evans & Lonsdale (1959).

references